

# Search for $\geq 400$ GeV gamma-rays from the SNR Cas A with the CAT telescope

P. Goret<sup>1</sup>, C. Gouiffes<sup>1</sup>, E. Nuss<sup>2</sup> (for the CAT collaboration), and D.C. Ellison<sup>3</sup>

<sup>1</sup>DSM, DAPNIA/SAP, CE Saclay, Gif-sur-Yvette, 91191, Cedex France

<sup>2</sup>Groupe de Physique Fondamentale, Université de Perpignan, Perpignan, 66860, France

<sup>3</sup>Department of Physics, North Carolina State University, Raleigh, NC 27695, USA

## Abstract

The recent detection of a hard X-ray component in the supernova remnant Cassiopeia A is interpreted as synchrotron emission from electrons accelerated to energies up to 40 TeV (Allen et al., 1997). It is therefore tempting to consider TeV gamma-ray emission from this object through : i) bremsstrahlung and inverse Compton radiation from electrons and/or ii)  $\pi^0$  production from an associated high energy cosmic ray component hitting surrounding material. Cas A was observed by the CAT imaging Cherenkov telescope during the observing season Aug-Nov 1998. An upper limit to the integral flux above 400 GeV of  $0.74 \times 10^{-11} \text{ } \gamma \text{ cm}^{-2} \text{ s}^{-1}$  is derived. This result is used to constrain shock-acceleration models for production of VHE gamma-rays in SNRs.

## 1 Introduction:

The supernova remnant Cassiopeia A (Cas A), aged  $\sim 300$  yr at a distance of  $\sim 2.8$  kpc, is the brightest radio source in the sky. The radio emission region is concentrated in a shell of radius  $\sim 130$  arcsec and thickness  $\sim 30$  arcsec. X-ray data from the RXTE satellite indicate the presence of electrons accelerated to energies up to  $\sim 40$  TeV which emit synchrotron photons above 10 keV (Allen et al., 1997). These electrons could generate  $\gamma$ -rays in the GeV-TeV band via inverse Compton or bremsstrahlung mechanisms. The  $\gamma$ -ray emissivity critically depends on the value of the magnetic field in the acceleration region. In addition, a nuclear component is likely to be accelerated along with electrons giving rise to additional  $\gamma$ -rays produced in nuclear collisions via  $\pi^0$  decay. Upper limits to the Cas A  $\gamma$ -ray flux above 100 MeV were obtained by the satellite experiments SAS-II and COS-B. Analyzing these data, Cowsik and Sarkar (1980) were able to set a lower limit of  $8 \times 10^{-5}$  G to the magnetic field in Cas A. Further observations by the EGRET experiment on the CGRO satellite led Esposito et al. (1996) to derive a more constraining lower limit of  $2 \times 10^{-4}$  G.

The situation in Cas A is reminiscent of that in SN1006 where Koyama et al. (1995) inferred the presence of up to 100 TeV electrons from the observed X-ray synchrotron emission. Subsequently, TeV  $\gamma$ -ray emission was observed by the CANGAROO atmospheric Cherenkov telescope (Tanimori et al., 1998). The Whipple collaboration, analyzing a 2.7 hr exposure on Cas A, reported an upper limit to the  $\gamma$ -ray flux above 300 GeV of  $2.6 \times 10^{-11} \text{ cm}^{-2} \text{ s}^{-1}$  (Lessard, 1996). More recently, the same group derived an improved upper limit of  $1.8 \times 10^{-11} \text{ cm}^{-2} \text{ s}^{-1}$  above 400 GeV from a 6.9 hr exposure (Lessard, 1999). In this paper, we present an analysis of a 24.4 hr exposure on Cas A obtained with the imaging atmospheric Cherenkov telescope CAT. The CAT telescope and the data analysis technique are described in section 2. The database is presented in section 3. The results of the analysis are summarized in section 4. The implications for current models of  $\gamma$ -ray production in SNR's are discussed in section 5.

## 2 The CAT telescope and data analysis:

The CAT imaging atmospheric Cherenkov telescope is described in Barrau et al. (1998). It consists of a  $18 \text{ m}^2$  Davies-Cotton mirror fitted with a 600 PMT fine-grained camera (pixel size:  $0.12^\circ$  diameter) at the focal plane. The energy threshold is 250 GeV at zenith. The telescope is located in the French Pyrénées at an altitude of 1650m and geographical coordinates  $2^\circ \text{ E}$ ,  $42^\circ \text{ N}$ . The data analysis technique used in the present paper is detailed in Le Bohec et al. (1998). The basis for the analysis of individual shower images is to compare the

observed image to a template of calculated images at different energies, zenith angles and impact parameters to the telescope. Gamma/hadron discrimination is performed with a cut on a single  $\chi^2$ -like parameter. The analysis also yields the energy, impact parameter and orientation (the equivalent of the  $\alpha$ -parameter in the standard Hillas method) for each event. Note that, in the present study, Cas A is considered as a point-like source, just as the Crab nebula is. Extensive Monte-Carlo simulations of the instrument have been performed and proved highly reliable when checked against real  $\gamma$ -rays from the Crab or Mkn501 (e.g. Goret, 1997, Mohanty, 1999).

### 3 The Cas A database:

The observations relevant for the present analysis were performed during the period August-November 1998. ON-source runs lasted for 30 minutes followed or preceded (but not systematically) by OFF-source runs shifted by  $\pm 35$  minutes in RA. After selection on meteorological conditions, zenith angle ( $\leq 25^\circ$ ) and correct experiment operation, a total exposure of 24.4 hr ON-source and 13.6 hr OFF-source were retained for further analysis. A database on the Crab nebula, with the same selection criteria and observing period, was also compiled to allow for cross-checking of the analysis. The trigger condition required that 4 PMTs above a threshold of 2.5 photoelectrons fire simultaneously within a sector (see Barrau et al., (1998), for details). The average raw trigger rate for these two data samples was  $\sim 17$  Hz. Both the Cas A and Crab data were processed the same way as is described in the next section.

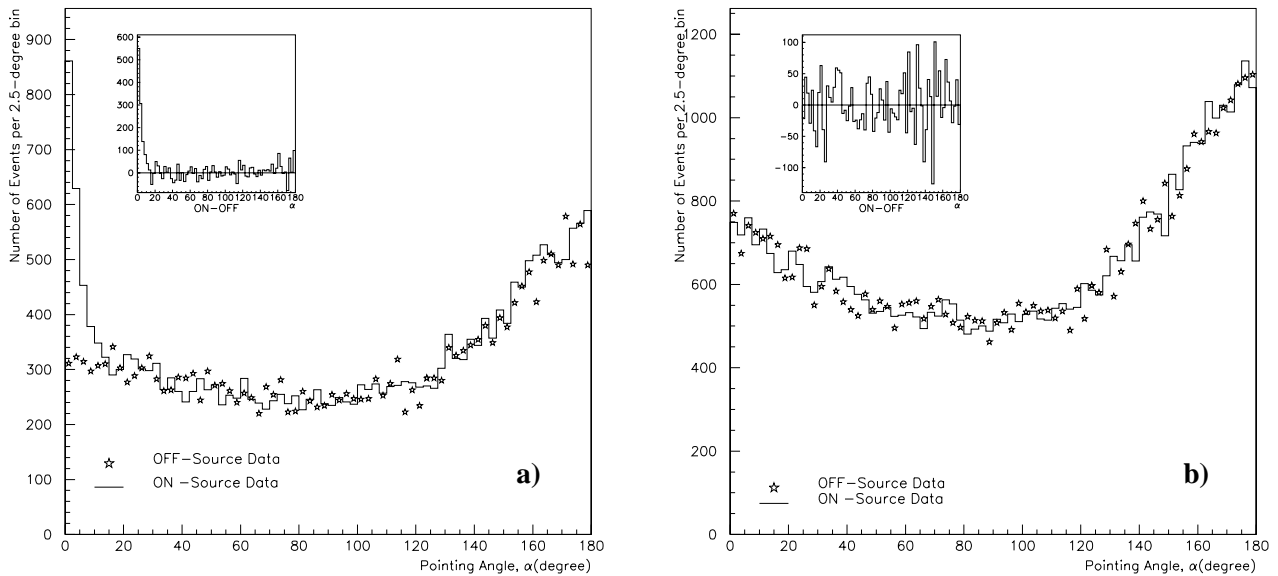


Figure 1: The distributions of the orientation angle  $\alpha$  for the Crab (a) and Cas A (b) datasets respectively using the  $\chi^2$  method. The ON and (renormalized) OFF-source data are represented by the solid histogram and stars respectively. The insets show the ON-OFF distributions. The data are binned in  $2.5^\circ$  intervals.

### 4 Results:

The Crab data were used to optimize the cuts for the best sensitivity in the search for a signal from Cas A. This analysis yielded the following cuts for gamma/hadron (shape) discrimination: i)  $\chi^2$  probability  $\geq 0.40$  and ii) a total number of photoelectrons in the image of  $Q_{\text{tot}} \geq 50$  p.e.. In addition, the estimated impact parameter was restricted to  $\leq 160$  m. The  $\alpha$ -plots for the Crab and Cas A are displayed in figure 1. The OFF data were

normalized using the tracking ratio, i.e., the ratio  $n_{\text{ON}}/n_{\text{OFF}}$  of the number of events surviving the shape cuts in the region  $20^\circ \leq \alpha \leq 120^\circ$ . The orientation cut was set to  $\alpha_{\text{max}}=8^\circ$ , which retains  $\sim 80\%$  of the  $\gamma$ -rays selected after the shape cuts according to Monte-Carlo simulations. The results of the analysis are summarized in Table 1.

	Crab	Cas A
$T_{\text{ON}}$ (hrs)	13.3	24.4
$T_{\text{OFF}}$ (hrs)	9.2	13.6
$N_{\text{ON}}$ (events)	2006	2360
$N_{\text{OFF}}$ (events)	706	1259
Tracking ratio	1.43	1.85
Excess (events)	998	33.5
Standard Deviation (events)	60.7	85.9
Significance ( $n_\sigma$ )	16.45	0.39

Table 1. *Results of the analysis for the Crab and Cas A.*

From these data, a  $3\sigma$  upper limit to the Cas A flux can be set at  $\leq 0.14$  times the Crab flux. Monte-Carlo calculations indicate that the energy threshold subsequent to the above cuts is 400 GeV, with  $\sim 89\%$  of the selected events in the sample having an effective energy above 400 GeV. The effective area, assuming a Crab-like energy spectrum for Cas A, is estimated to be  $\sim 3.5 \times 10^8 \text{cm}^2$ . With the assumption of a null detected signal, this translates into a  $3\sigma$  upper limit to the Cas A  $\gamma$ -ray flux of:

$$\Phi(\geq 400 \text{ GeV}) \leq 0.74 \times 10^{-11} \gamma \text{cm}^{-2} \text{s}^{-1}$$

The implications of this result concerning the current models for TeV-gamma production in SNRs are examined in the next section.

## 5 Discussion:

As was already noted by Cowsik and Sarkar (1980), considering  $\gamma$ -ray production via bremsstrahlung and inverse Compton, upper limits on the  $\gamma$ -ray flux from Cas A must constrain primarily the strength of the magnetic field in the source. The problem was recently reconsidered by Baring et al. (1999) using a non-linear shock-acceleration model. The model aims at predicting the overall continuum photon emission spectrum in SNRs from radio to  $\gamma$ -rays. The model was tailored to the specific case of Cas A by Ellison et al (1999), taking into account relevant observations over the full photon energy range. The results are displayed in figure 2, which shows the best fit of the model to the data from radio through X-rays up to  $\gamma$ -rays. The contributions of the different components (synchrotron, bremsstrahlung, IC and p-p) in each energy band are indicated. The conclusion is that in order to account for the upper limits reported in both the GeV and TeV ranges, the strength of the magnetic field must be greater than  $\sim 10^{-3} \text{G}$ . As discussed by Cowsik and Sarkar (1980), such a high value in excess of the equipartition field of  $\sim 4 \times 10^{-4} \text{G}$  calls for a magnetohydrodynamic field amplification which remains to be fully investigated (see Keohane, (1998), for a recent discussion). The present result may also be considered in the frame of the diffusive shock-acceleration model of Drury, Aharonian and Völk (1994) as a test of cosmic-ray acceleration in SNRs.

## 6 Conclusions:

The improved upper limit to the TeV  $\gamma$ -ray flux from the SNR Cas A presented in this paper sets a stringent lower limit to the magnetic field in the acceleration region. This result should help understanding the mechanisms at work in this young object.

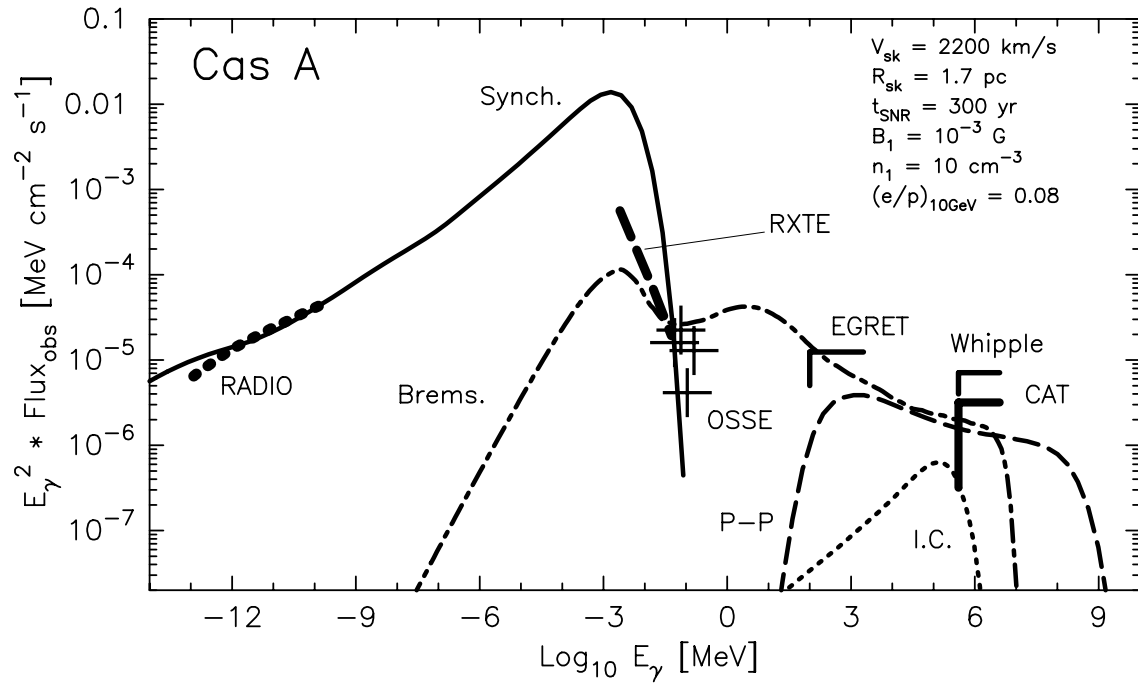


Figure 2: Predictions of the nonlinear diffusive shock-acceleration model from radio to TeV  $\gamma$ -rays as compared to observations (see Ellison et al. (1999) for details and references therein). The present result is shown together with the Whipple upper limit of Lessard (1999).

## References

- Allen, G.E., et al. 1997, ApJ 487, L97  
 Baring, M.G., et al. 1999, ApJ 513, 311  
 Barrau, A., et al. 1998, Nucl. Instr. Meth. A 416, 278  
 Cowsik, R., & Sarkar, S. 1980, MNRAS 191, 855  
 Drury, L.O'C. et al. 1994, A& A 287, 959  
 Ellison, D.C., et al. 1999, this conference OG 2.2.09  
 Goret, P. 1997, Proc. Kruger TeV Workshop on Gamma-Ray Astrophysics, p.166  
 Keohane, J.W. 1998, PhD thesis, University of Minnesota  
 Koyama, K., et al. 1995, Nature 378, 255  
 Le Bohec, S., 1998, Nucl. Instr. Meth. A 416, 425  
 Lessard, R. 1996, PhD thesis, Purdue University  
 Lessard, R. 1999, Proc. 19th Texas Symposium, Paris 1998, in press  
 Mohanty, G. 1999, this conference OG 2.2.03  
 Tanimori, T., et al. 1998, ApJ 497, L25